Research Square

Preprints are preliminary reports that have not undergone peer review.
They should not be considered conclusive, used to inform clinical practice,
or referenced by the media as validated information.

Effects of closed-loop BCI-triggered iTBS over the DLPFC on upper-limb Motor and cognitive recovery after stroke: a randomized controlled trial

Yan Gong

gongyan@njmu.edu.cn

The Affiliated Suzhou Hospital of Nanjing Medical University, Suzhou Rehabilitation Hospital, Suzhou Municipal Hospital, Gusu School

Meilin Liu

The Affiliated Suzhou Hospital of Nanjing Medical University, Suzhou Rehabilitation Hospital, Suzhou Municipal Hospital, Gusu School

Chunyu Li

National University of Singapore

Juan Li

The Affiliated Suzhou Hospital of Nanjing Medical University, Suzhou Rehabilitation Hospital, Suzhou Municipal Hospital, Gusu School

Rentao Zhang

The Affiliated Suzhou Hospital of Nanjing Medical University, Suzhou Rehabilitation Hospital, Suzhou Municipal Hospital, Gusu School

Yajing Lan

The Affiliated Suzhou Hospital of Nanjing Medical University, Suzhou Rehabilitation Hospital, Suzhou Municipal Hospital, Gusu School

Surong Qian

The Affiliated Suzhou Hospital of Nanjing Medical University, Suzhou Rehabilitation Hospital, Suzhou Municipal Hospital, Gusu School

Research Article

Keywords: Stroke, Brain-computer interface, Intermittent theta-burst stimulation, Upper limb motor function

Posted Date: November 18th, 2026

DOI: https://doi.org/10.21203/rs.3.rs-11452392/v1

License: This work is licensed under a Creative Commons Attribution 4.0 International License.
Read Full License

Additional Declarations: No competing interests reported.

Title Page

Article type： Original Article

Title: Effects of closed-loop BCI-triggered iTBS over the DLPFC on upper-limb Motor and cognitive recovery after stroke: a randomized controlled trial

Order of Authors：

Yan Gong[1#*]

Meilin Liu[1,2#]

Chunyu Li[3#]

Juan Li[1]

Rentao Zhang[1]

Yajing Lan[1,2]

Surong Qian[*]

1 Department of Rehabilitation medicine, The Affiliated Suzhou Hospital of Nanjing Medical University, Suzhou Rehabilitation Hospital, Suzhou Municipal Hospital, Gusu School, Suzhou, Jiangsu, 215000, China.

2 College of Health-Preservation and Wellness, Dalian Medical University, Liaoning, Dalian, 116044, China.

3. Department of Biomedical Engineering, College of Design and Engineering, National University of Singapore, Singapore

[#] These authors contributed equally to this work.

*Correspondences: Yan Gong, gongyan@njmu.edu.cn. Surong Qian, qiansurong8@gmail.com.

【Abstract】

Background: Stroke frequently causes persistent upper-limb motor and cognitive impairment. Although brain–computer interface (BCI) training combined with transcranial magnetic stimulation may promote post-stroke neuroplasticity, the effects of brain-state-dependent closed-loop stimulation remain unclear. This study aimed to evaluate the effects of closed-loop BCI-triggered intermittent theta-burst stimulation (iTBS) targeting the ipsilesional dorsolateral prefrontal cortex (DLPFC) on upper-limb and cognitive recovery after stroke, and to explore the underlying neural mechanisms using electroencephalography (EEG).

Methods: Participants were randomly allocated (1:1:1) to Control, BCI–sham, or BCI–iTBS. The BCI–iTBS group received real-time BCI-synchronized iTBS over ipsilesional DLPFC across 12 sessions within two weeks. The BCI–sham group underwent identical BCI training with sham iTBS. The control group only received standard rehabilitation. Clinical assessments were performed at baseline, post-intervention, and 4-week follow-up. Resting-state, motor imagery, motor attempt, and P300 EEG recordings were collected.

Results: Of 72 enrolled, 71 completed the trial. All groups improved clinically ($p<0.05$). The BCI–iTBS group achieved significantly greater gains in upper-limb motor function and cognition than control and BCI–sham groups ($p<0.05$). Neurophysiologically, the BCI-iTBS group showed a significant pre-to-post reduction in theta-band resting-state connectivity between the contralesional frontal and contralesional occipital regions. During affected-hand motor imagery, changes in the alpha-band ERD laterality index

differed between the BCI-Sham and BCI-iTBS groups. Moreover, the BCI-iTBS group showed a directional shift toward zero, consistent with a more balanced cortical activation pattern. No significant differences in change scores were observed for P300 amplitude or latency.

Conclusions: Closed-loop BCI-triggered iTBS of the DLPFC promotes upper-limb motor and cognitive recovery after stroke and modulates brain network reorganization and neuroplasticity, representing a promising therapeutic strategy for post-stroke neurorehabilitation.

Trial registration: This study was registered in the Chinese Clinical Trial Registry (ChiCTR2500095965).

Keywords: Stroke, Brain-computer interface,Intermittent theta-burst stimulation,Upper limb motor function

Background

Stroke remains a leading cause of death and long-term disability worldwide [1, 2]. Approximately 60% of stroke survivors present with upper extremity (UE) motor deficits at onset, and 55–75% still experience persistent functional limitations at three to six months post-stroke [3, 4]. Upper limb recovery is generally less favorable than lower limb recovery, posing a major clinical challenge [5, 6]. Developing effective rehabilitative strategies for post-stroke upper limb recovery has therefore become an urgent priority in neurorehabilitation.

Post-stroke motor recovery depends on neuroplasticity and interhemispheric reorganization [7, 8]. Non-invasive brain stimulation (NIBS), particularly transcranial magnetic stimulation (TMS), has been widely applied in post-stroke rehabilitation. Intermittent theta-burst stimulation (iTBS), a modified TMS protocol, induces longer-lasting neural effects with shorter duration and lower intensity than conventional TMS [12, 13]. Current TMS treatment for stroke is mainly based on the interhemispheric inhibition (IHI) model, which posits that motor recovery involves rebalancing interhemispheric inhibition and corticomotor excitability [14, 15]. However, significant interindividual variability exists in post-stroke brain function, and not all changes conform to the IHI model [16]. This variability partly explains why TMS remains controversial in terms of optimal parameters and clinical outcomes. Evidence suggests that TMS over the primary motor cortex (M1) may promote upper-limb recovery, but effects vary considerably across individuals [15, 17]. Such variability is closely linked to the overall excitability state of cortical networks after stroke [18], suggesting that brain state-dependent TMS protocols may improve therapeutic efficacy.

Brain-computer interface (BCI) technology decodes motor intention signals to control external devices while providing visual or tactile feedback, establishing bidirectional brain-computer interaction [19, 20]. The feasibility and efficacy of BCI interventions in promoting motor recovery and cortical plasticity have been demonstrated [20]. However, approximately 40% of stroke survivors cannot control BCI effectively, resulting in low decoding accuracy [21, 22]. Event-related desynchronization (ERD) and event-related synchronization (ERS) reflect cortical

activation and inhibition, respectively. Studies show that 15–30% of healthy participants exhibit BCI illiteracy, primarily due to failure to generate effective ERD in the mu rhythm (8–30 Hz) over the motor cortex, leading to poor BCI decoding accuracy [27-29]. Therefore, enhancing ERD is crucial for improving BCI performance. iTBS over the affected M1 increases cortical excitability for 20–30 min and enhances sensorimotor ERD [12, 13]. However, sequential iTBS with BCI did not significantly improve BCI performance [30]. Furthermore, iTBS applied to M1 does not significantly improve BCI accuracy or facilitate neuroplastic changes following BCI training [21], suggesting that M1 may not be an optimal stimulation target for enhancing BCI performance. In contrast, iTBS over the right dorsolateral prefrontal cortex (DLPFC) has been shown to improve motor imagery (MI)-BCI training outcomes and may mitigate BCI inefficiency [31]. Thus, the DLPFC represents a more promising target for modulating motor imagery and optimizing BCI systems.

We therefore propose a brain state-dependent, closed-loop iTBS protocol triggered by a BCI system in stroke patients. We hypothesize that this approach can deliver iTBS to the affected DLPFC in real time according to the patient‘s brain state, thereby enabling closed-loop neuromodulation that enhances neuroplasticity and facilitates upper-limb motor recovery. To test this hypothesis, we conducted a randomized, double-blind, controlled study to evaluate the safety and clinical efficacy of closed-loop BCI-triggered iTBS in stroke patients, and to investigate its neural mechanisms using multiple electroencephalogram (EEG) assessment paradigms.

Methods

Patient recruitment

This was a randomized, double-blind, controlled trial conducted at Suzhou Municipal Hospital and Suzhou Rehabilitation Hospital. Patients were eligible if they had: (1) clinically confirmed ischemic or hemorrhagic stroke by computerized tomography (CT) or magnetic resonance imaging (MRI), (2) stroke onset between 2 weeks and 6 months, with unilateral upper-limb motor dysfunction, (3) Fugl-Meyer Assessment for upper extremity (FMA-UE) score < 66, (4) Mini-mental state examination (MMSE) score $\geq$ 20, and (5) ability to cooperate with motor imagery tasks and electroencephalogram (EEG) acquisition. Exclusion criteria were: (1) coexisting other central or peripheral nervous system disorders; (2) non-stroke-related organic upper extremity injuries, (3) severe aphasia or comprehension deficits impeding rehabilitation training, or poor compliance, (4) intracranial metallic implants, cardiac pacemaker, or unrepaired skull defect contraindicating MRI, and (5) recent participation in other clinical trials.

The study was approved by the Ethics Committee of Suzhou Municipal Hospital (Approval No. J-2025-020-K01) and registered prospectively with the Chinese Clinical Trial Registry (ChiCTR2500095965). This study was conducted in accordance with the Declaration of Helsinki. All participants or their immediate legal guardians provided written informed consent.

Study design

A total of 72 eligible patients were enrolled and randomly allocated (1:1:1) to the control, BCI–sham, or BCI–iTBS group using a computer-generated random sequence. Outcome evaluators were blinded to group allocation and interventions. Clinical assessments were conducted at baseline (T0), immediately post-intervention (T1), and at 4-week follow-up (T2).

Electroencephalogram (EEG) neurophysiological assessments were conducted at baseline and immediately post-intervention (T1). The study flowchart is shown in **Figure 1.**

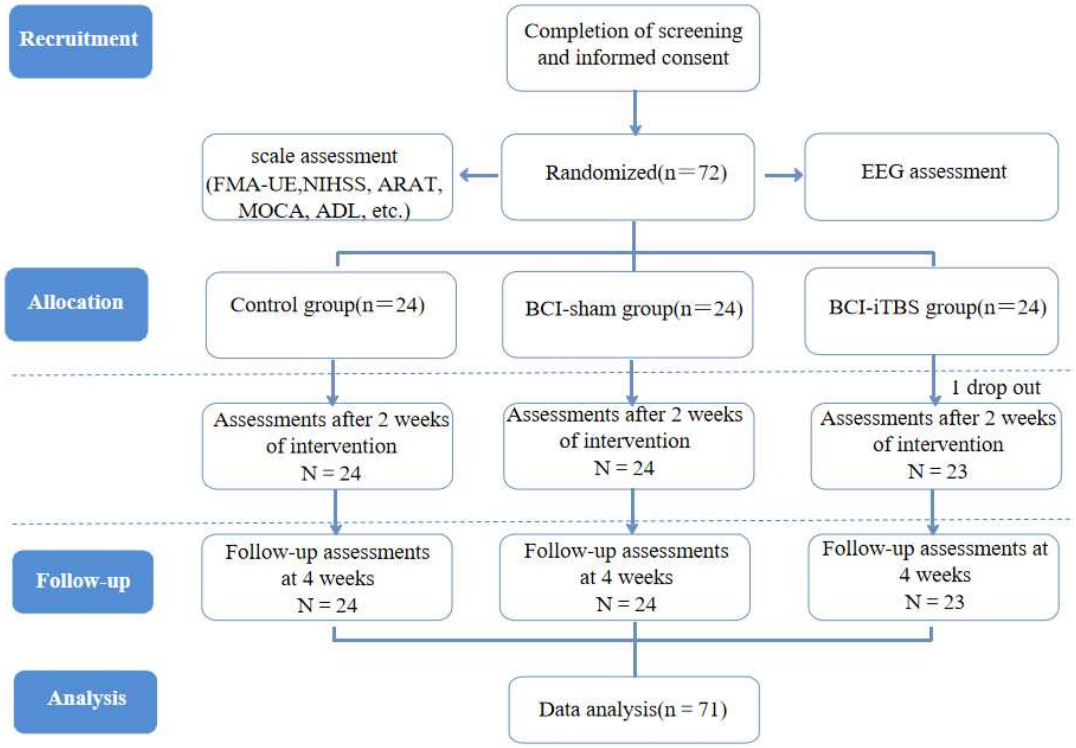


Figure 1. Flow diagram of the study

Intervention

Overall rehabilitation program. All participants received standard rehabilitation during the 2-week intervention phase, including physical therapy (range of motion, muscle strengthening, and balance training), occupational therapy (activities of daily living and task-specific training), and coordination exercises. In addition, each group received a supplementary 30-minute session daily for 12 sessions (6 sessions/week over 2 weeks). Total rehabilitation time and intensity were matched across groups.

Closed-loop BCI-triggered iTBS. The closed-loop BCI-triggered iTBS protocol combined a TMS system (MagproR30, MagVenture, Denmark) synchronized with a BCI system (Shanghai Idea Interaction Technology Co., Ltd., Shanghai, China) (Figure

2A–C). A 32-channel 10–20 EEG cap and wireless amplifier sampled EEG at 500 Hz for online motor-intention decoding during visually cued grasp-release motor imagery (Figure 2D). Once sensorimotor rhythm (8–30 Hz) ERD was detected, the BCI system triggered iTBS bursts over the ipsilesional DLPFC (Figure 2E). The TMS coil was positioned over the ipsilesional DLPFC at 45°to the midline to induce posterior-anterior current flow. Stimulation intensity was set at 110% resting motor threshold. Each triggered iTBS burst contained five pulses at 50 Hz.

Each BCI–iTBS session comprised five blocks of 30 trials (Figure 2F). At T = 0 s, a fixation cross appeared. At T = 2 s, simultaneous brief tactile stimuli were applied to both hands as a preparatory cue. At T = 3 s, a red square appeared as an imperative cue, prompting participants to perform motor imagery of left- or right-hand grasping and opening movements (side randomized across trials). Participants were instructed to imagine performing the movements as vividly and rapidly as possible, repeating the action until the fixation cross disappeared. The red square disappeared at T = 4.5 s, and the fixation cross remained visible until T = 8 s. At T = 8 s, upon successful online decoding of motor intention, a burst of iTBS was delivered to the ipsilesional DLPFC. Participants then rested for 10 s before the next trial. Each session lasted approximately 30 minutes, with simultaneous EEG recording under resting-state, motor imagery, and motor attempt paradigms.

The BCI–sham group underwent identical BCI training, visual feedback, and ERD-based triggering; however, the magnetic stimulation coil was placed perpendicular to the scalp over the same DLPFC site to deliver sham stimulation without real cortical

activation, preserving comparable auditory and somatosensory perception. The control group received standard rehabilitation only during the supplementary sessions. All groups completed 12 supplementary sessions over two weeks with matched total intervention dosage. The full experimental timeline is illustrated in **Figure 2.**

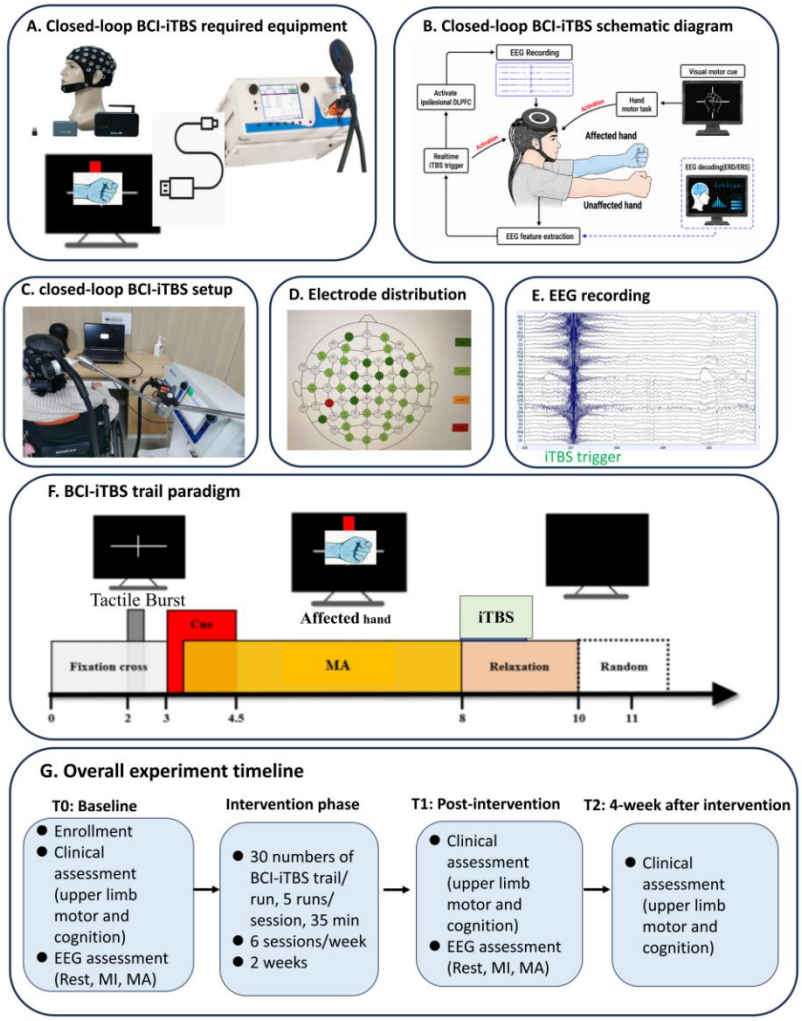


Figure 2. Closed-loop BCI-iTBS intervention protocol and experimental procedures. (A) Equipment required for closed-loop BCI-iTBS. (B) Schematic diagram of closed-loop BCI-iTBS; EEG signals from the affected motor cortex triggered iTBS delivery to the ipsilesional DLPFC upon detection of motor intent. (C) Closed-loop BCI-iTBS setup, showing a participant seated in front of a screen with EEG electrodes and a TMS coil positioned over the ipsilesional hemisphere. (D) Distribution of EEG electrodes. (E) EEG recording. (F) Timeline of a single BCI-iTBS trial. (G) Overall experimental procedure.

Clinical assessments

Clinical assessments were conducted at T0, T1, and T2 by trained physiotherapists blinded to group allocation. The primary outcome was the change in upper extremity motor function assessed by FMA-UE (66 points), including FMA-shoulder/elbow (42 points), FMA-wrist (10 points), FMA-hand (14 points), and FMA-coordination and speed (6 points). Secondary outcomes included the NIHSS for neurological impairment severity; the ARAT for upper limb and hand function; the SAFE for synergistic motor recovery; the FTHUE-HK for upper limb functional recovery level; the Modified Barthel Index for ADL independence; and the MoCA for cognitive function.

EEG Acquisition, Preprocessing, and Analysis

EEG recording and experimental paradigms

MI and MA are widely used to assess motor-system engagement in post-stroke BCI research[12, 32]. EEG data were acquired at T0 and T1 using an iRecorder W32 amplifier (Shanghai Idea Interaction Technology Co., Ltd., Shanghai, China). Electrode impedance was maintained below 5 kΩ, and EEG was band-pass filtered 1-100 Hz and digitized at 500 Hz. Each assessment included one eyes-open resting-state recording followed by four motor-task blocks in the fixed order MI-MA-MI-MA, followed by P300 recording. The resting-state block was always collected first to avoid potential carryover effects from motor tasks. Participants were instructed to remain relaxed, keep their eyes open, fixate on a cross, and avoid speaking or intentional movements.

For MI and MA tasks, stimuli were presented by E–Prime 3.0 (Psychology Software Tools, Pittsburgh, PA, USA), with event markers synchronized to EEG acquisition. Each MI or MA block comprised 40 trials, including 20 trials per hand in randomized order. A fixation cross

appeared at trial onset. A bilateral tactile cue was delivered at 2 s, followed by a motor cue at 3 s. The motor cue was labelled S1 or S2 according to the instructed hand. It disappeared at 4.5 s, while the fixation cross remained visible until the end of the motor period at 8 s. During MI, participants imagined repeated grasping-and-opening movements of the cued hand. During MA, they attempted the same movement to the best of their residual motor ability. The inter-trial interval varied randomly from 2.5 to 4.5 s.

For the P300 task, the recorded S1 and S2 event classes were used to define target and standard trials, respectively. Therefore, the P300 was based on the event markers present in each EEG recording.

EEG preprocessing and lesion-side normalization

EEG preprocessing and reporting followed recommendations for reproducible EEG research[33]. EEG data were processed in MATLAB R2025a (MathWorks, Natick, MA, USA) using EEGLAB functions[34]. Continuous EEG was band-pass filtered from 0.5 to 30 Hz. Independent component analysis (ICA) was then applied to separate reproducible neural and artifact-related components[35]. Components classified by ICLabel as ocular artifacts with a probability of at least 0.80 were removed[36]. The cleaned resting-state and motor-task datasets were resampled to 250 Hz. Offline re-referencing used T7 and T8 as the reference pair; these channels were excluded from connectivity analyses.

For lateralized task analyses, recordings from patients with left-hemisphere lesions were spatially normalized by exchanging homologous left- and right-sided channel labels. This aligned the affected hemisphere across participants, whereas midline electrodes remained unchanged. The normalization was applied only to analyses involving affected/ipsilesional and

224 unaffected/contralesional comparisons; non-lateralized resting-state and P300 measures
225 retained their original sensor labels.

226 **Resting-state spectral and connectivity analysis**

227 Resting-state power spectral density (PSD) was estimated using Welch's method with 2-s
228 windows and 50% overlap[37]. PSD was expressed in decibels. Occipital spectral activity was
229 characterized using O1, Oz, and O2; Oz was also retained as a single-electrode measure.
230 Posterior-midline PSD was calculated from Pz and Oz.

231 Band-averaged PSD topographies and connectivity analyses focused on theta (4-8 Hz), alpha
232 (8-13 Hz), and beta (13-30 Hz) activity. Bilateral ROI definitions are provided in following
233 Table.

ROI	Node	
	Left	Right
Frontal	Fp1, AF3, F7, F3, FC1	Fp2, AF4, F8, F4, FC2
Central	FC5, C3, CP1, CP5	FC6, C4, CP2, CP6
Parietal	P7, P3	P4, P8
Occipital	PO3, O1	PO4, O2

234 Functional connectivity was quantified using the weighted phase-lag index (wPLI), which
235 reduces the influence of zero-lag coupling associated with volume conduction [38]:

236 $$wPLI_{xy} = \frac{|\mathrm{E}[\mathrm{Im}(S_{xy})]|}{\mathrm{E}[|\mathrm{Im}(S_{xy})|]}$$

237 where S_{xy} denotes the complex cross-spectrum between electrodes (x) and (y), $\mathrm{Im}(\cdot)$
238 denotes the imaginary component, and $\mathrm{E}[\cdot]$ denotes averaging across observations. For each
239 frequency band, EEG was band-pass filtered and divided into overlapping 2-s windows. The

analytic signal was derived using the Hilbert transform. Pairwise wPLI was calculated within each window and then averaged across windows. ROI-to-ROI wPLI was summarized as the median of all available channel-pair values between the corresponding ROI sets. Within-ROI and between-ROI channel pairs were retained for targeted connectivity matrices.

Motor-task time-frequency, ERD, laterality, and connectivity analyses

Motor-task EEG was epoched from −3 s to 8 s relative to the S1/S2 motor cue. The interval from −1.75 to −0.25 s served as the baseline. Time-frequency analysis was performed from 1 to 30 Hz using a continuous wavelet transform. For each trial and channel, the squared magnitude of the wavelet coefficients was used as the power estimate. Power was averaged across trials within each recording before baseline normalization and logarithmic transformation[39]:

$$ERSP(f,t) = 10\log_{10}\left(\frac{\bar{P}(f,t)}{\bar{P}_{\text{base}}(f)}\right)$$

where $\bar{P}(f,t)$ denotes the trial-averaged power at frequency (f) and time (t), and $\bar{P}_{\text{base}}(f)$ denotes the corresponding trial-averaged baseline power at frequency (f). Negative ERSP values indicate event-related desynchronization (ERD), whereas positive values indicate event-related synchronization (ERS)[40]. Wavelet analysis was selected because it characterizes frequency-specific temporal changes in non-stationary EEG signals[41, 42].

The primary task interval was defined as 1.5-5.0 s after cue onset. Group-average ERSP was visualized at C3, Cz, and C4. Alpha- and beta-band scalp topographies were calculated by averaging ERSP values across this task interval.

For ERD laterality analysis, task-to-baseline linear power ratios were calculated separately for the contralesional and ipsilesional central ROIs. A normalized ERD laterality index was calculated as[24]:

$$\mathrm{LI}_{\mathrm{ERD}} = \frac{R_{\mathrm{contra}} - R_{\mathrm{ipsi}}}{R_{\mathrm{contra}} + R_{\mathrm{ipsi}}}$$

where R_{contra} and R_{ipsi} denote the contralesional and ipsilesional task-to-baseline power ratios, respectively. A positive value indicates relatively stronger ERD in the ipsilesional central region.

Task-related wPLI was calculated over the same 1.5-5.0-s interval in the alpha and beta bands, using the estimator defined in the resting-state connectivity analysis. For each comparison, wPLI values were averaged across unique channel pairs within an ROI or between the relevant pair of ROIs.

P300 ERP and time-frequency analysis

P300 epochs were extracted separately for target and standard events from −200 to 800 ms relative to event onset. Each epoch was baseline corrected using the −200 to 0 ms interval. At Pz, ERPs were averaged separately for target and standard trials. The target-minus-standard difference waveform was calculated as:

$$ERP_{\mathrm{diff}}(t) = ERP_{\mathrm{target}}(t) - ERP_{\mathrm{standard}}(t)$$

where ERP_target (t)and ERP_standard (t) denote the target- and standard-trial ERP amplitudes at time (t), respectively. P300 amplitude and latency were quantified from the difference waveform within the 300-600 ms interval, which encompasses the typical temporal range of the P3b component[43, 44].

Time-frequency representations were also calculated at Pz for target and standard trials using the ERSP procedure described in motor task. Target-minus-standard ERSP maps were obtained by subtracting the standard-trial ERSP from the target-trial ERSP at each time-frequency point and were used to visualize intervention-related changes in stimulus-locked spectral activity.

Statistical Analysis

Statistical analyses were performed in SPSS 24.0. For measurements satisfying normality and homogeneity–of–variance assumptions, the mean ± standard deviation was used to represent them. Subsequently, repeated–measures analysis of variance (ANOVA) was applied, with group as the between–subject factor and time as the within–subject factor, and LSD-corrected multiple comparison methods to analyze the data. Additionally, for the measurement data and rating data that did not follow a normal distribution, the median (interquartile range) was used for expression, and the independent samples Kruskal-Wallis test was used to compare these data.

In the analysis of EEG signals, each analysis included participants who had complete pre-intervention and post-intervention EEG recordings that were matched. The final paired sample comprised 20 Control participants, 17 BCI-Sham participants, and 19 BCI-iTBS participants for resting-state analyses. For motor-task analyses, the corresponding sample sizes were 21, 18, and 15 for MI, and 21, 18, and 13 for MA, respectively. P300 analyses included 19 Control participants, 16 BCI-Sham participants, and 13 BCI-iTBS participants. Within-group pre/post differences in scalar EEG measures were assessed using paired tests. For each measure (X), the change score was calculated as:

$$\Delta X = X_{\mathrm{Post}} - X_{\mathrm{Pre}}$$

Between-group differences in change scores were evaluated using one-way analysis of variance, followed by pairwise Welch's t-tests. For the resting-state ROI wPLI matrices, paired pre/post tests were conducted separately for each edge, and ΔwPLI values were compared across groups using one-way analysis of variance. To account for multiple edge-wise tests, the Benjamini-Hochberg procedure was applied across the 28 unique connections within each frequency band; $q < 0.05$ was considered statistically significant [45]. Pixel-wise ERSP change maps were evaluated using paired tests, with uncorrected $P < 0.05$ displayed as significant pixels.

Results

Participant flow and baseline characteristics

A total of 72 participants were enrolled and randomly assigned to the control (n = 24), BCI–sham (n = 24), and BCI–iTBS (n = 24) groups. One participant in the BCI–iTBS group withdrew, leaving 71 participants who completed the study (control, n = 24; BCI–sham, n = 24; BCI–iTBS, n = 23). Baseline demographic and clinical characteristics were balanced across the three groups (all $p > 0.05$; Table 1). No device-related adverse events, intervention intolerance, or serious adverse events were reported during the study period.

Table 1. The demographic and baseline clinical characteristics of three groups

Variables	Control group	BCI-sham group	BCI-iTBS group	*P*-values
N	24	24	23	
Gender (Male/Female)	17/7	15/9	15/8	0.824
Age (years)	60.33 ± 13.45	54.71 ± 12.85	59.43 ± 12.06	0.271
Time since stroke (days)	30.83 ± 7.69	34.75 ± 9.75	29.61 ± 11.59	0.175
Type of stroke (infract/hemorrhage)	17/7	16/8	19/4	0.443
Paretic limb (left/right	12/12	15/9	8/15	0.164
HMFSS	0.50 (0.00, 1.75)	0.00 (0.00, 1.00)	1.00 (0.00, 1.00)	0.246
FMA-UE	16.50 (8.75, 26.50)	12.50 (7.00, 20.00)	14.00 (6.00, 26.00)	0.563
FMA-SA	14.50 ± 7.30	12.96 ± 7.75	11.74 ± 5.64	0.401
FMA-Wrist	2.00 (0.00, 4.00)	0.00 (0.00, 3.00)	2.00 (0.00, 4.00)	0.399
FMA-Hand	0.00 (0.00, 2.00)	0.00 (0.00, 0.00)	2.00 (0.00, 2.00)	0.136
FMA-Coordination	0.00 (0.00, 1.00)	0.00 (0.00, 1.50)	0.00 (0.00, 3.00)	0.67
FTHUEHK	2.50 (1.25, 3.00)	2.00 (1.00, 3.00)	2.00 (1.00, 3.00)	0.675
ARAT	0.00 (0.00, 7.25)	0.00 (0.00, 5.50)	2.00 (0.00, 9.00)	0.649
SAFE	2.96 ± 2.12	2.58 ± 1.59	2.65 ± 1.67	0.748
ADL	52.00 (36.75, 64.25)	45.00 (35.75, 55.00)	50.00 (40.00, 70.00)	0.503
MEP	576.00 (456.25, 724.00)	643.90 (530.50,740.75)	596.50 (510.00-879.00)	0.456
CMCT	8.83 ± 0.928	9.07 ± 1.47	9.12 ± 1.29	0.683
MOCA	23.00 (21.00, 25.75)	24.00 (21.00, 25.00)	23.00 (22.00, 25.00)	0.902

Table 1.The demographic and baseline clinical characteristics of three group. NIHSS, National Institutes of Health Stroke Scale;FMA-UE, Fugl–Meyer Assessment of Upper Extremity; FMA-SA, Fugl-Meyer Assessment for Shoulder/Arm; FMA-Wrist, Fugl-Meyer assessment for wrist; FMA-Hand , Fugl-Meyer assessment for hand ; FMA-Coordination ,FMA-coordination motor scores ; FTHUEHK, Functional Test for the Hemiplegic Upper Extremity in Hong Kong; ARAT, Action Research Arm Test; SAFE ,Shoulder Abduction and Finger Extension score;ADL , Daily living activities; MEP ,Motor evoked potential; CMCT ,Central Motor Conduction Time; MOCA ,Montreal Cognitive Assessment.

Clinical outcomes

Clinical outcomes were assessed immediately post-intervention (T1) and at 4-week follow-up (T2). Post-treatment scores and change scores (Δ) for all groups are presented in Tables 2-3 and Figure 3.

Table 2. Changes in upper-limb motor and cognitive function scores from baseline among three groups after interventions

Variables	POST			Change scores from baseline			
	Control group	BCI-sham group	BCI-iTBS group	Control group	BCI-sham group	BCI-iTBS group	
	Mean ± SD	Mean ± SD	Mean ± SD	Median difference (95% CI)	Median difference (95% CI)	Median difference (95% CI)	*P* -values
N	24	24	23	24	24	23	
NIHSS	1.00 (1.00, 2.00)	0.00 (0.00,2.00)[a]	2.00 (2.00, 3.00)[bc]	1.00 (0.48,0.94)	0.00 (0.06, 0.52)[a]	1.00 (0.93, 1.51)[bc]	<0.001
FMA-UE	19.50 (12.50, 31.75)	16.50 (9.25, 25.75)	35.00 (17.00, 40.00)[bc]	3.00 (2.75, 5.00)	2.00 (2.47, 6.20)	11.00 (10.08, 18.18)[bc]	<0.001
FMA-SA	17.21 ± 7.18	16.04 ± 8.63	21.09 ± 7.57[c]	2.00 (2.01, 3.41)	2.00 (1.80, 4.36)	8.00 (6.97, 11.73)[bc]	<0.001
FMA-Wrist	3.00 (0.50, 4.00)	0.00 (0.00, 3.00)	3.00 (2.00,4.00)[c]	0.00 (0.04, 0.79)	0.00 (-0.16, 0.58)	0.00 (0.69, 2.36)[bc]	0.01
FMA-Hand	0.00 (0.00, 2.75)	0.00 (0.00, 1.50)	2.00 (0.00, 5.00)[c]	0.00 (-0.15, 0.73)	0.00 (-0.07, 0.49)	0.00 (0.44, 2.35)[c]	0.091
FMA-Coordination	0.00 (0.00, 2.75)	0.00 (0.00, 2.00)	3.00 (0.00, 5.00)[bc]	0.00 (-0.03, 0.78)	0.00 (-0.30, 0.80)	1.00 (0.84, 2.55)[bc]	0.003
FTHUEHK	3.00 (2.00, 4.00)	2.00 (2.00, 4.00)	4.00 (3.00, 4.00)[c]	1.00 (0.54, 1.21)	0.50 (0.32, 1.09)	1.00 (1.22, 1.99)[bc]	<0.001
ARAT	5.00 (0.25, 11.75)	0.00(0.00, 13.75)	9.00 (3.00, 17.00)[c]	1.50 (1.26, 4.24)	0.00 (0.25, 4.83)	6.00 (4.39, 13.35)[bc]	<0.001
SAFE	4.00 (2.00, 7.00)	3.00 (2.00, 5.00)	5.00 (3.00, 7.00)[c]	1.00 (0.97, 1.61)	1.00 (0.45, 1.38)[a]	2.00 (1.71, 2.89)[bc]	<0.001
ADL	55.00 (46.25, 80.00)	55.50 (40.50, 79.50)	75.00 (55.00, 85.00)[c]	8.00 (6.91, 13.68)	5.50 (4.64, 14.78)	15.00 (11.47, 21.66)[bc]	0.008
MOCA	23.25 ± 2.58	24.33 ± 2.50	25.04 ± 1.67[b]	0.29 (0.1, 0.49)	1.25 (0.89, 1.61)[a]	1.65 (1.27, 2.03)[b]	<0.001

Table 2. Changes in upper-limb motor and cognitive function scores from baseline among three groups after intervention. a:Control group VS BCI-sham group ; b:Control groupVS BCI-iTBS group; c: BCI-sham group VS BCI-iTBS group NIHSS, National Institutes of Health Stroke Scale;FMA-UE, Fugl–Meyer Assessment of Upper Extremity; FMA-SA, Fugl-Meyer Assessment for Shoulder/Arm; FMA-Wrist, Fugl-Meyer Assessment for wrist; FMA-Hand , Fugl-Meyer Assessment for hand ; FMA-Coordination ,Fugl-Meyer Assessment for coordination ; FTHUEHK, Functional Test for the Hemiplegic Upper Extremity in Hong Kong; ARAT, Action Research Arm Test; SAFE ,Shoulder Abduction and Finger Extension score; ADL , Daily living activities;MOCA ,Montreal Cognitive Assessment. NIHSS, National Institutes of Health Stroke Scale; FMA-UE, Fugl–Meyer Assessment of Upper Extremity; FMA-SA, Fugl-Meyer Assessment for Shoulder/Arm; FMA-Wrist, Fugl-Meyer Assessment for wrist; FMA-Hand, Fugl-Meyer Assessment for hand; FMA-Coordination, Fugl-Meyer Assessment for coordination ; FTHUEHK, Functional Test for the Hemiplegic Upper Extremity in Hong Kong; ARAT, Action Research Arm Test; SAFE ,Shoulder Abduction and Finger Extension score; ADL, Daily living activities;MOCA ,Montreal Cognitive Assessment.

Table 3. Changes in upper-limb motor and cognitive function scores from baseline among three groups at 4-week follow-up

Variables	Four weeks post			Change scores from baseline			
	Control group	BCI-sham group	BCI-iTBS group	Control group	BCI-sham group	BCI-iTBS group	
	Mean ± SD	Mean ± SD	Mean ± SD	Median difference (95% CI)	Median difference (95% CI)	Median difference (95% CI)	*P* -values
N	24	24	23	24	24	23	
NIHSS	1.50 (1.00, 2.75)	1.00 (1.00, 2.75)	3.00 (2.00, 3.00)[bc]	1.00 (0.67, 1.16)	1.00 (0.67, 1.25)	2.00 (1.52, 2.04)[bc]	<0.001
FMA-UE	21.50 (15.25, 37.25)	17.00 (12.00, 28.50)	39.00 (22.00, 47.00)[bc]	6.00 (5.08, 9.09)	4.00 (4.01, 8.24)[a]	18.00 (15.75, 23.55)[bc]	<0.001
FMA-SA	19.00 (13.50, 25.50)	15.00 (12.00, 21.00)	27.00 (17.00, 30.00)[bc]	5.00 (4.01, 6.57)	4.00 (3.02, 5.73)	13.00 (10.58, 15.16)[bc]	<0.001
FMA-Wrist	3.00 (0.50, 4.00)	1.50 (0.00, 3.75)	4.00 (3.00, 6.00)[bc]	0.00 (0.13, 0.87)	0.00 (0.17, 0.91)	3.00 (1.74, 3.39)[bc]	<0.001
FMA-Hand	0.00 (0.00, 3.00)	0.00 (0.00, 1.50)	3.00 (1.00, 6.00)[bc]	0.00 (0.05, 0.87)	0.00 (-0.01, 0.68)	2.00 (1.14, 2.95)[bc]	<0.001
FMA-Coordination	0.00 (0.00, 2.75)	0.00 (0.00, 3.00)	3.00 (2.00, 5.00)[bc]	0.00 (-0.06, 0.90)	0.00 (0.04, 1.12)	2.00 (1.14, 2.94)[bc]	<0.001
FTHUEHK	3.00 (2.25, 4.00)	3.00 (2.00, 4.75)	5.00 (4.00, 6.00)[bc]	1.00 (0.81, 1.36)	1.00 (0.77, 1.48)	2.00 (1.84, 2.76)[bc]	<0.001
ARAT	5.50 (0.50, 14.00)	2.00 (0.00, 16.00)	14.00 (7.00, 30.00)[bc]	3.00 (2.19, 5.89)	2.00 (1.01, 6.66)	9.00 (8.30, 17.79)[bc]	<0.001
SAFE	4.00 (2.25, 8.00)	3.50 (3.00, 5.75)	6.00 (5.00, 8.00)[bc]	1.50 (1.22, 2.03)	1.00 (0.99, 1.92)	3.00 (2.67, 4.11)[bc]	<0.001
ADL	58.00 (49.75,82.75)	58.00 (44.25, 82.25)	82.00 (65.00, 92.00)[bc]	10.50 (9.36, 16.22)	10.00 (8.52, 18.39)	20.00 (17.70,29.51)[bc]	<0.001
MOCA	23.54 ± 2.45	24.88 ± 2.58[b]	25.65 ± 1.72	0.50 (0.31,0.86)	1.50 (1.31,2.27)	2.00 (1.89,2.63)[b]	<0.001

Table 3. Changes in upper-limb motor and cognitive function scores from baseline among three groups at 4-week follow-up. The remaining abbreviations are the same as those in Table 2.

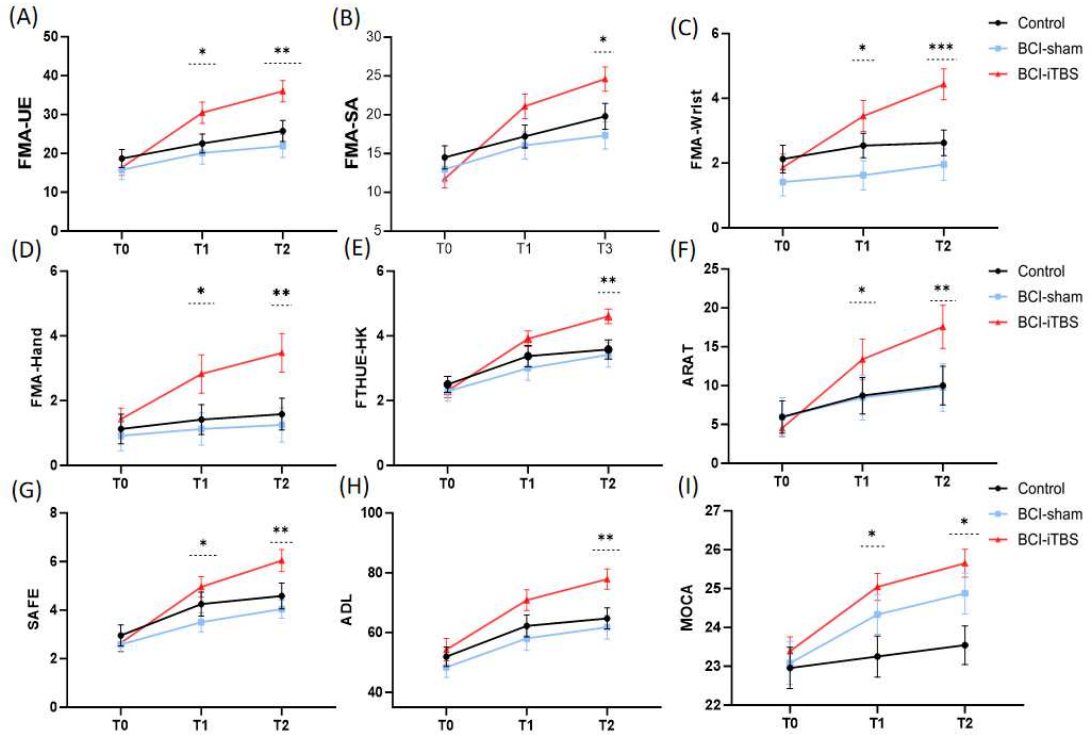


Figure 3. Improvements in upper-limb motor and cognitive function scores in baseline(T0), post-intervention (T1) and follow-up (T2) . Control = control group, BCI-sham = BCI-sham group, BCI-iTBS BCI-iTBS group. FMA-UE, Fugl-Meyer assessment for the upper extremity; FMA-SA, Fugl-Meyer Assessment for Shoulder/Arm; FMA-wrist, Fugl-Meyer Assessment for Wrist; FMA-Hand, Fugl-Meyer Assessment for hand; FTHUEHK, Functional Test for the Hemiplegic Upper Extremity in Hong Kong; ARAT, Action Research Arm Test; SAFE, Shoulder Abduction and Finger Extension score; ADL,Daily living activities;MOCA ,Montreal Cognitive Assessment. * $p < 0.05$, ** $p < 0.01$, *** $p < 0.001$.

Primary outcome

For the primary outcome, FMA-UE, a significant between-group difference was observed at T1 ($p < 0.001$). Post hoc comparisons showed that the BCI–iTBS group improved significantly more than both the control and BCI–sham groups (both $p < 0.001$), with no difference between the latter two ($p = 0.650$). At T2, the between-group difference persisted ($p < 0.001$), with the BCI–iTBS group continuing to show greater improvements than both control and BCI–sham groups (both $p < 0.001$), and no difference between control and BCI–sham ($p > 0.05$).

Secondary outcomes after intervention (T1)

At T1, significant between-group differences were observed for all secondary measures except FMA-Hand (all $p < 0.05$). For ΔFMA-SA ($p < 0.001$), ΔFMA-Wrist ($p = 0.010$), and ΔFMA-Coordination ($p = 0.003$), the BCI–iTBS group showed significantly greater improvements than both control and BCI–sham groups (all $p < 0.05$), with no differences between control and BCI–sham. For ΔFMA-Hand, the overall test was not significant ($p = 0.091$); however, exploratory pairwise comparisons indicated that BCI–iTBS outperformed both control ($p = 0.001$) and BCI–sham ($p < 0.001$), with no difference between the latter two ($p = 0.532$). For ΔFTHUE-HK ($p < 0.001$), ΔARAT ($p < 0.001$), ΔSAFE ($p < 0.001$), and ΔADL ($p = 0.008$), the BCI–iTBS group yielded greater improvements than both control and BCI–sham groups (all $p < 0.05$), with no differences between control and BCI–sham (all $p > 0.05$). For ΔMoCA ($p < 0.001$) and ΔNIHSS ($p < 0.001$), all three groups differed significantly from each other, with the BCI–iTBS group showing the largest improvement, followed by BCI–sham, and then control (all $p < 0.01$).

Secondary outcomes at 4-week follow-up（T2)

At T2, significant between-group differences were sustained for all variables (all $p < 0.001$; Table 3). For ΔFMA-UE, ΔFMA-SA, ΔFMA-Wrist, and ΔFMA-Coordination (all $p < 0.001$), the BCI–iTBS group continued to show significantly greater improvements than both control and BCI–sham groups (all $p < 0.001$), with no differences between control and BCI–sham (all $p > 0.05$). For ΔFMA-Hand ($p < 0.001$), BCI–iTBS outperformed both control ($p = 0.001$) and BCI–sham ($p < 0.001$), while

control and BCI–sham did not differ ($p = 0.532$). For all secondary motor and functional outcomes at T2 (ΔFTHUE-HK, ΔARAT, ΔSAFE, ΔADL), the BCI–iTBS group demonstrated significantly greater improvements than both control and BCI–sham groups (all $p \leq 0.001$), with no significant differences between control and BCI–sham groups (all $p > 0.05$). For ΔNIHSS at T2, BCI–iTBS also showed superior neurological recovery over both control and BCI–sham groups (both $p < 0.001$), while control and BCI–sham did not differ ($p = 0.843$). The overall between-group difference for ΔMoCA at T2 was also significant ($p < 0.001$).

Brain–Function Changes in the Three Groups

3.4 Brain function changes in the three groups

3.4.1 Resting-state EEG spectral power and functional connectivity

Resting-state EEG spectral power and theta-band functional connectivity are shown in **Figure 4**. At the unadjusted level, the change in this connection differed across groups ($F(2,53) = 5.28$, $p = 0.008$, $\eta^2 = 0.166$). The BCI-iTBS group showed a larger decrease than the Control group ($\Delta = 0.034 \pm 0.104$; $p = 0.002$) and the BCI-Sham group ($\Delta = 0.016 \pm 0.104$; $p = 0.018$). However, no between-group ROI-wPLI difference remained significant after correction across the full set of ROI connections. The group-average PSD curves and scalp topographies are presented in **Figure 4A and 4B.**

In the BCI-iTBS group, theta-band connectivity between the contralesional frontal and contralesional occipital ROIs decreased from Pre (0.125 ± 0.070) to Post (0.066 ± 0.051; $\Delta = -0.058 \pm 0.066$; $t(18) = -3.83$, $p = 0.001$, BH-FDR-adjusted $q = 0.035$; Table 4). This connection remained significant after correction for the ROI-wise

comparisons and is shown in the theta-band wPLI matrix (**Figure 4C**).

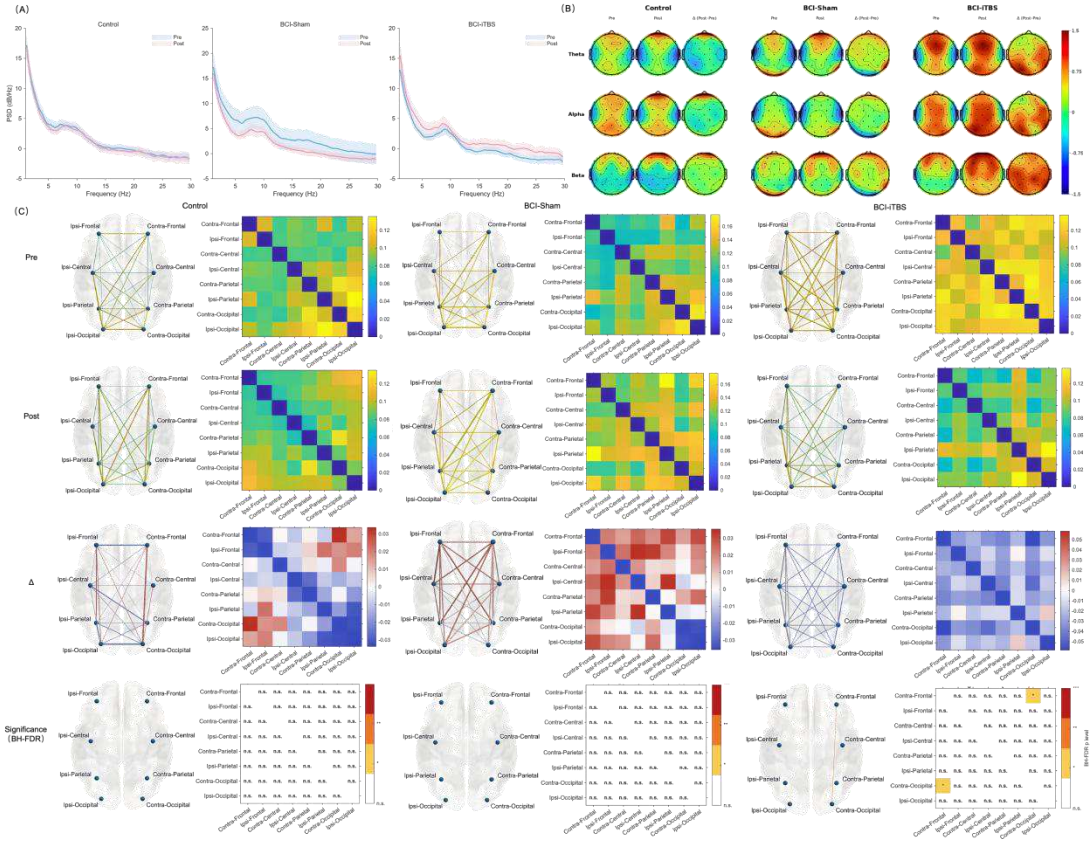


Figure 4. Resting-state spectral power and theta-band functional connectivity. (A) Group-average PSD at Oz before (Pre) and after (Post) intervention. Shaded areas indicate the standard error of the mean. (B) Band-averaged PSD topographies in the theta, alpha, and beta bands, shown for Pre, Post, and Δ (Post–Pre). (C) Theta-band ROI-level wPLI networks and matrices at Pre and Post, together with Δ wPLI and statistical maps. Significant connections were determined at $q < 0.05$ after Benjamini–Hochberg false discovery rate correction.

3.4.2 Motor imagery task

MI-related time–frequency activity, laterality indices, functional connectivity, and scalp topographies are shown in **Figure 5**. During affected-hand MI, ipsilesional central beta-band ERD became more negative in the BCI-Sham group, changing from −1.31 ± 0.61 dB at Pre to −1.68 ± 0.62 dB at Post (Δ = −0.37 ± 0.54 dB; $t(17) = -2.87$, $p = 0.011$). This change differed from that in the Control group (Δ = 0.15 ± 0.69 dB; $p = 0.013$; Table 4). The corresponding time–frequency and scalp distributions are shown in

Figure 5A and 5D.

The contralesional central beta-band ERD change also differed between the Control ($\Delta = 0.10 \pm 0.44$ dB) and BCI-Sham groups ($\Delta = -0.45 \pm 1.04$ dB; $p = 0.049$). In addition, the alpha-band ERD laterality-index change differed between the BCI-Sham ($\Delta = 0.053 \pm 0.144$) and BCI-iTBS groups ($\Delta = -0.041 \pm 0.111$; $p = 0.045$); the laterality-index comparisons are shown in **Figure 5B.**

Alpha-band central interhemispheric wPLI during affected- and unaffected-hand MI is shown in **Figure 5C**. During affected-hand MI, no significant within-group Pre/Post change was observed (all $p \geq 0.301$), and change scores did not differ among groups ($F(2,51) = 0.205$, $p = 0.815$). In contrast, the change in wPLI during unaffected-hand MI differed among groups ($F(2,51) = 3.198$, $p = 0.049$). The BCI-Sham group showed a negative mean change score ($\Delta = -0.027 \pm 0.070$), whereas the Control ($\Delta = 0.025 \pm 0.074$) and BCI-iTBS groups ($\Delta = 0.041 \pm 0.108$) showed positive mean change scores. Post-hoc comparisons showed differences between the BCI-Sham and Control groups ($p = 0.028$) and between the BCI-Sham and BCI-iTBS groups ($p = 0.045$; **Table 4**).

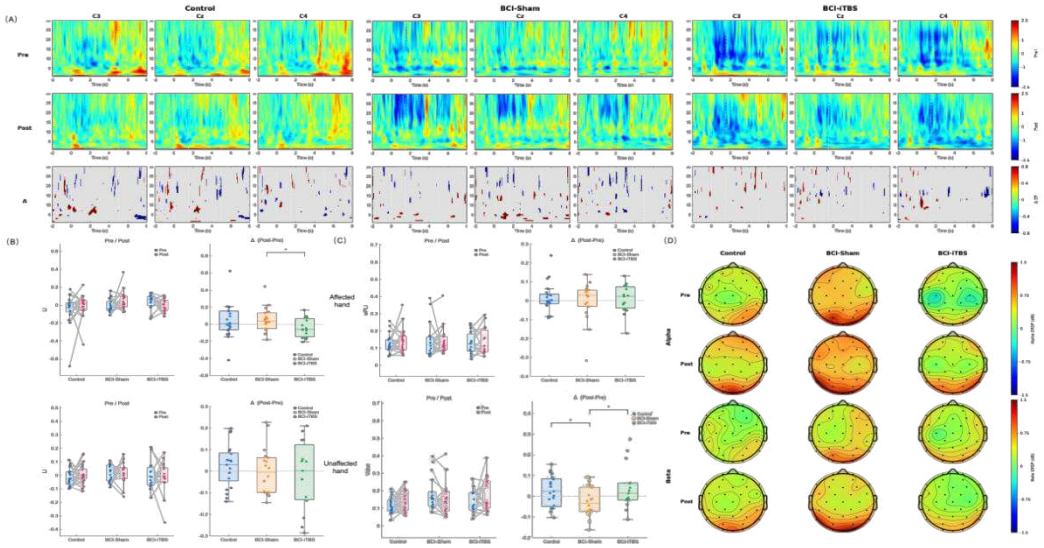


Figure 5. Motor-imagery (MI) task-related time–frequency activity, lateralization, functional connectivity, and scalp topographies. (A) Group-average ERSP at C3, Cz, and C4 before treatment (Pre), after treatment (Post), and for the paired change (Δ, Post−Pre). (paired-test *p* < 0.05); gray pixels are non-significant. (B) Pre/Post comparisons and change-score distributions for selected lateralization indices (LI) during affected- and unaffected-hand MI. (C) Pre/Post comparisons and change-score distributions of alpha-band central interhemispheric weighted phase-lag index (wPLI) during affected-hand MI (top) and unaffected-hand MI (bottom). Paired observations are shown in the left panels, and group distributions of change scores are shown in the right panels. Brackets and asterisks indicate significant between-group comparisons of Δ values ($p < 0.05$). (D) Alpha- and beta-band task-related scalp topographies during affected-hand MI at Pre and Post.

3.4.3 Motor attempt task

MA-related time–frequency activity, ERD laterality, central connectivity, and scalp topographies are shown in **Figure 6A–D**. During affected-hand MA, the beta-band ERD laterality-index change differed between the Control ($\Delta = -0.017 \pm 0.114$) and BCI-Sham groups ($\Delta = 0.069 \pm 0.142$; $p = 0.047$); the laterality-index comparison is shown in **Figure 6B.**

Interhemispheric central alpha-band wPLI decreased in the BCI-Sham group from 0.157 ± 0.097 at Pre to 0.121 ± 0.069 at Post ($\Delta = -0.036 \pm 0.068$; $t(17) = -2.25$, $p = 0.038$; Table 4); the corresponding connectivity comparison is shown in **Figure 6C**. The change in interhemispheric central alpha-band wPLI differed among groups ($F(2,49) = 5.89$, $p = 0.005$). Post-hoc comparisons indicated that the BCI-Sham group differed from the Control group (Control $\Delta = 0.023 \pm 0.059$; $p = 0.007$) and the BCI-iTBS group (BCI-iTBS $\Delta = 0.034 \pm 0.066$; $p = 0.008$).

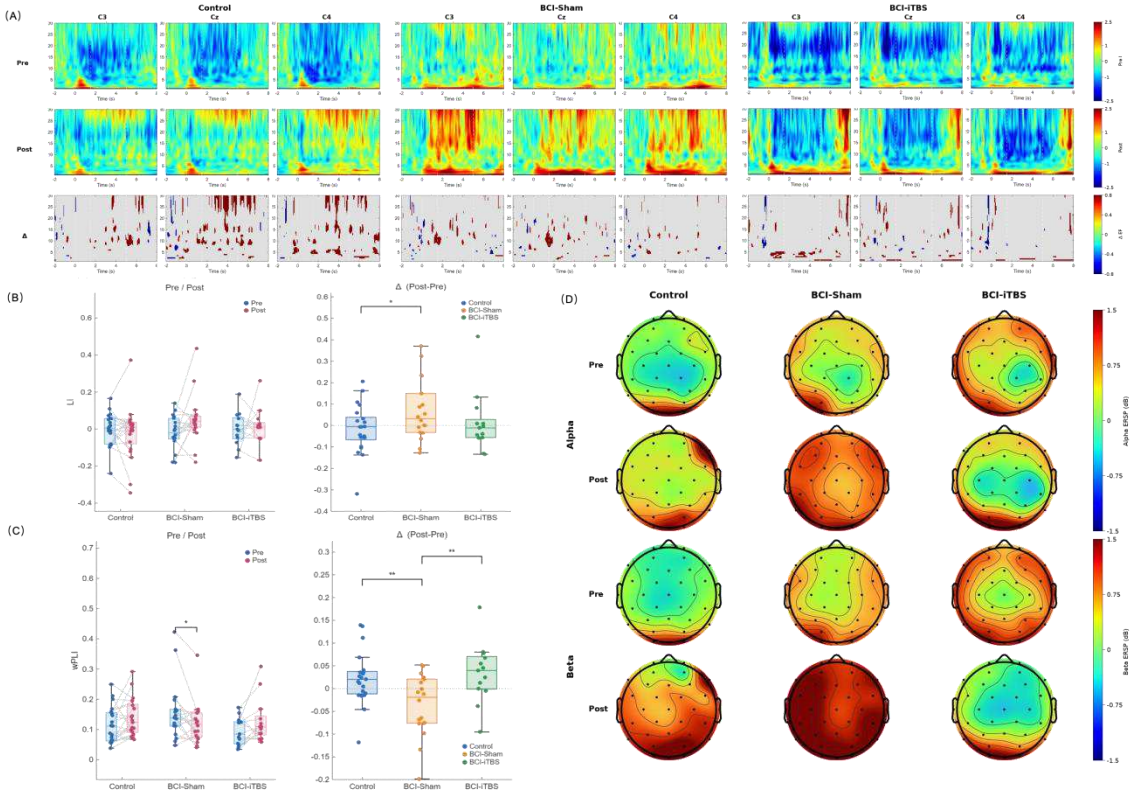


Figure 6. Motor attempt (MA) results during affected-hand movement. (A) Group-average ERSPs at C3, Cz, and C4 before (Pre) and after (Post) intervention, and paired change maps (Δ, Post–Pre). Coloured pixels in the Δ maps indicate uncorrected paired t-test results at $p < 0.05$; grey pixels are non-significant. (B) Pre/Post comparisons and between-group comparisons of change scores in the β-band ERD lateralization index (LI) for the bilateral central region. (C) Pre/Post comparisons and between-group comparisons of change scores in α-band interhemispheric wPLI between the left and right central regions. (D) Scalp topographies of task-related ERSP in the α and β bands. Boxplots show medians and interquartile ranges; dots represent individual participants and connecting lines indicate paired observations. Brackets and asterisks indicate significant between-group comparisons of Δ values ($p < 0.05$; *$p < 0.01$).

3.4. P300 ERP and time–frequency results during cognitive task

Target-minus-standard Pz ERP waveforms and time–frequency maps are shown in **Figure 7(A, B)**, respectively. No within-group pre/post changes were observed in P300 difference-wave amplitude (Control, $p = 0.458$; BCI-Sham, $p = 0.920$; BCI-iTBS, $p = 0.444$) or latency (Control, $p = 0.086$; BCI-Sham, $p = 0.281$; BCI-iTBS, $p = 0.385$). Change scores did not differ among groups for either amplitude ($p = 0.779$) or latency ($p = 0.904$; Table 4).

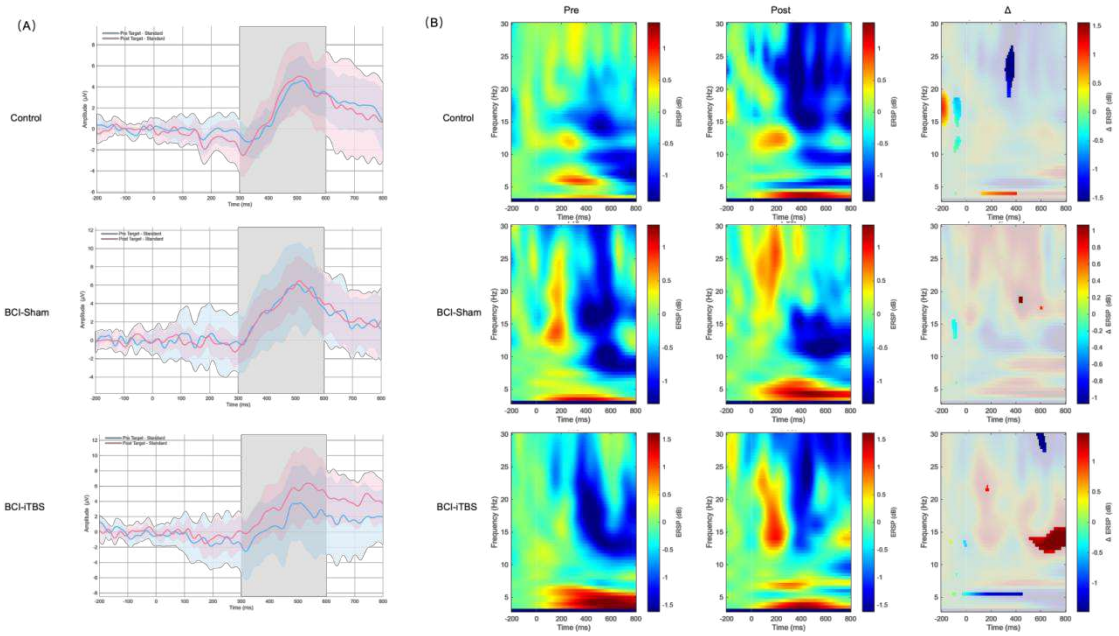


Figure 7. P300 event-related potential and time–frequency responses at Pz. (A) Group-average Pz waveforms elicited by target and standard stimuli before (Pre) and after (Post) intervention. The grey band marks the P300 analysis window. (B) Pz target-minus-standard ERSPs at Pre and Post, together with the paired change maps (Δ, Post–Pre). Coloured pixels in the Δ maps indicate paired t-test results at $p < 0.05$; grey areas are non-significant.

Task	Outcome	Group	Pre	Post	Δ	Within-group *p*	Between-group comparison of Δ
Rest	Theta wPLI: contralesional frontal–contralesional occipital	Control	0.077 ± 0.051	0.110 ± 0.118	0.034 ± 0.104	0.165	F(2,53)=5.276, *p* =0.008; iTBS vs Control, *p* =0.002; iTBS vs Sham, *p* =0.018
		BCI-Sham	0.086 ± 0.073	0.102 ± 0.069	0.016 ± 0.104	0.527	
		BCI-iTBS	0.125 ± 0.070	0.066 ± 0.051	−0.058 ± 0.066	0.001*	
MI, affected hand	Ipsilesional central beta ERD (dB)	Control	−1.258 ± 0.551	−1.104 ± 0.445	0.153 ± 0.692	0.322	Control vs BCI-Sham: *p* = 0.013*
		BCI-Sham	−1.311 ± 0.612	−1.676 ± 0.618	−0.365 ± 0.539	0.011*	
		BCI-iTBS	−1.442 ± 0.840	−1.985 ± 1.876	−0.543 ± 2.021	0.316	
	Contralesional central beta ERD (dB)	Control	−1.273 ± 0.356	−1.174 ± 0.427	0.099 ± 0.444	0.318	Control vs BCI-Sham: *p* = 0.049*
		BCI-Sham	−1.496 ± 0.692	−1.944 ± 1.077	−0.447 ± 1.037	0.085	
		BCI-iTBS	−1.472 ± 0.767	−1.804 ± 1.588	−0.332 ± 1.834	0.494	
MA, affected hand	Alpha ERD laterality index	Control	−0.049 ± 0.172	−0.011 ± 0.125	0.038 ± 0.200	0.391	BCI-Sham vs BCI-iTBS: *p* = 0.045*
		BCI-Sham	−0.006 ± 0.074	0.047 ± 0.108	0.053 ± 0.144	0.140	
		BCI-iTBS	0.039 ± 0.086	−0.001 ± 0.070	−0.041 ± 0.111	0.181	
	Interhemispheric central alpha wPLI	Control	0.116 ± 0.060	0.138 ± 0.062	0.023 ± 0.059	0.090	F(2,49)=5.892, *p* =0.005; Control vs Sham, *p* =0.007; Sham vs iTBS, *p* =0.008
		BCI-Sham	0.157 ± 0.097	0.121 ± 0.069	−0.036 ± 0.068	0.038*	
		BCI-iTBS	0.095 ± 0.046	0.129 ± 0.074	0.034 ± 0.066	0.086	
P300 at Pz	Beta ERD laterality index	Control	−0.003 ± 0.089	−0.020 ± 0.143	−0.017 ± 0.114	0.496	Control vs BCI-Sham: *p* = 0.047*
		BCI-Sham	−0.017 ± 0.090	0.051 ± 0.132	0.069 ± 0.142	0.056	
		BCI-iTBS	0.001 ± 0.090	0.014 ± 0.098	0.013 ± 0.141	0.742	
	Target-minus-standard amplitude (μV)	Control	7.061 ± 4.448	8.716 ± 8.011	1.656 ± 9.517	0.458	Overall: *p* = 0.779
		BCI-Sham	8.997 ± 8.461	8.742 ± 5.760	−0.256 ± 9.951	0.920	
		BCI-iTBS	7.235 ± 8.065	9.236 ± 7.387	2.001 ± 9.107	0.444	
	Target-minus-standard latency (ms)	Control	520.947 ± 60.463	491.053 ± 63.845	−29.895 ± 71.794	0.086	Overall: *p* = 0.904
		BCI-Sham	492.375 ± 58.983	472.750 ± 70.415	−19.625 ± 70.223	0.281	
		BCI-iTBS	513.692 ± 71.939	493.077 ± 79.806	−20.615 ± 82.395	0.385	

Table 4. Summary of the main EEG outcomes. Values are mean ± SD. Δ = Post–Pre. Negative ERD values indicate desynchronization. Within-group comparisons used paired tests; change scores were compared across groups using one-way analysis of variance and Welch's t tests where

appropriate. All p values are two-sided. For the resting-state ROI-wPLI matrix, the BCI-iTBS frontal–occipital within-group change remained significant after BH-FDR correction ($q = 0.035$); no between-group edge was retained after correction. *$p < 0.05$.

Discussion

In this study, we investigated the potential synergistic effects of synchronous BCI-triggered iTBS targeting the ipsilesional DLPFC in patients with stroke. Our results showed that this closed-loop intervention significantly improved post-stroke upper-limb motor function, particularly proximal shoulder and elbow movements, and produced measurable cognitive benefits related to attention. The therapeutic efficacy exceeded that of BCI training alone or standard rehabilitation. Neurophysiological evidence further indicated that the combined intervention enhanced ERD over the ipsilesional sensorimotor cortex during motor imagery of the affected hand and promoted a shift in the lateralization of motor-related cortical activation toward a more normal pattern, suggesting enhanced neural plasticity and functional reorganization.

Some stroke patients cannot effectively control a BCI as reduced cortical excitability together with cognitive and attentional impairments leads to low BCI decoding accuracy [46]. Previous studies have shown that NIBS can activate the motor cortex and improve BCI performance [22]. Several studies combining rTMS with BCI training in stroke survivors reported restored interhemispheric balance and improved BCI decoding accuracy when rTMS was applied as preconditioning before BCI practice [26, 48]. Afonso et al. further reported that sequential bilateral rTMS paired with virtual reality-supported BCI yielded clinical motor gains and increased sensorimotor ERD amplitude in chronic stroke patients [49]. Nevertheless, sequential

BCI combined with TMS paradigms have notable intrinsic limitations. Conventional rTMS delivers stimulation at fixed timings regardless of ongoing brain states, so pulses may be delivered during periods of low cortical excitability with insufficient ERD, reducing the efficiency of plasticity induction. To overcome this drawback, ERD-triggered closed-loop BCI–TMS paradigms have been proposed, in which stimulation is released only upon detection of effective MI-related ERD signals. Gharabaghi et al. used real-time ERD-triggered TMS during MI and achieved greater cortical excitability enhancement in stroke patients than non-triggered stimulation [50]. Daly et al. further demonstrated that corticospinal excitability dynamically varies with ERD magnitude and peaks within a specific ERD window that fixed-timing protocols frequently miss [51]. Therefore, an ERD-triggered closed-loop BCI–TMS paradigm can capture excitatory brain states during MI and enhance the efficiency of plasticity induction for post-stroke upper-limb rehabilitation.

The frontoparietal network is the core neural substrate for motor imagery, in which the DLPFC acts as a critical hub [52–56]. Anodal tDCS or high-frequency rTMS over the DLPFC can facilitate motor imagery performance, whereas DLPFC inhibition produces opposite effects [56]. In stroke patients, strong functional connectivity is observed between the DLPFC and premotor cortex during MI tasks [57]. Modulating DLPFC excitability thus represents a promising strategy to enhance BCI rehabilitation outcomes. Based on recent research, we propose for the first time a brain state-dependent real-time closed-loop iTBS strategy targeting the DLPFC and triggered by a BCI system for decoding motor intention.

Consistent with our primary hypothesis, the BCI–iTBS group achieved superior clinical improvements relative to the control and BCI–sham groups. The mean increase in FMA-UE

score reached 21 points post-intervention and 25 points at 4-week follow-up, both far exceeding the widely accepted minimal clinically important difference of 5 points [58]. Moreover, the magnitude of improvement was significantly greater than that reported in previous studies of BCI alone, iTBS alone, or sequential BCI–iTBS training, supporting a synergistic interaction between the two interventions [12, 59–61]. However, no significant between-group difference was found in the ΔFMA-Hand score after intervention, which may be attributable to the proximal-to-distal gradient of upper-limb motor recovery and the relatively short intervention duration.

We observed a significant decrease in resting-state theta-band functional connectivity between the contralesional frontal and contralesional occipital regions after DLPFC iTBS. This aligns with prior fMRI observations that DLPFC-targeted iTBS suppresses redundant synchronization within and between the default mode network and frontoparietal network in healthy participants [62]. Such connectivity reduction did not lead to cognitive deterioration but instead mitigated internal mental distraction and improved task processing efficiency. Since the DLPFC is a core node within motor imagery networks, and effective connectivity from the supplementary motor area to the DLPFC predicts MI performance [63], these findings suggest that DLPFC iTBS may specifically modulate the functional connectivity of motor imagery-related brain networks, potentially by suppressing redundant cross-regional synchronization and thereby optimizing network efficiency.

Our results showed that BCI feedback significantly enhanced beta-band ERD over the ipsilesional central region during affected-hand MI, with a comparable trend over the contralesional hemisphere, indicating bilateral cortical recruitment for neural compensation.

Previous studies have shown that bilateral sensorimotor ERD during affected-hand MI is inversely correlated with the FMA-UE score of the affected upper extremity [64, 65], suggesting that stronger ipsilesional ERD is associated with milder motor impairment. However, the role of contralesional ERD remains controversial. Some investigations reported higher contralesional ERD in patients with more severe motor deficits, interpreted as compensatory activation recruited to compensate for damaged ipsilesional circuits [66, 67]. Whether elevated contralesional ERD is causally linked to motor impairment requires further verification.

The ERD laterality index reflects the hemispheric balance of cortical activation, with values near zero representing bilateral, balanced activation. Healthy individuals exhibit dominant contralateral cortical activation during unilateral hand movements [68], and LI values approaching zero correlate with better upper-limb functional recovery after stroke [69, 70]. In the present study, alpha-band ERD LI changed divergently across groups during affected-hand MI. The BCI-sham group displayed further contralesional hemisphere dominance, exacerbating the compensatory pattern. In contrast, the BCI–iTBS group shifted LI toward zero, shifting activation from bilateral or contralesional dominance toward ipsilesional predominance, a pattern more consistent with the normal activation profile observed in healthy individuals.

During the MA task, the BCI–sham group exhibited a significant reduction in alpha-band central interhemispheric wPLI, whereas no comparable change was observed during the MI task. This suggests that MA is more effective than MI in driving cortical functional connectivity remodeling, consistent with previous reports showing higher BCI classification accuracy and broader network engagement for MA tasks [65]. Despite identical BCI motor feedback tasks, the BCI-iTBS group did not exhibit the same task-dependent compensatory

electroencephalographic changes under concurrent neuromodulation. The discrepancy between groups may stem not only from treatment modality but also from differences in lesion severity. Although all lesions were localized in the basal ganglia, the BCI–sham group had more severe damage, necessitating compensatory plasticity of the contralesional hemisphere during training. In comparison, patients receiving closed-loop BCI-triggered iTBS could better engage the ipsilesional hemisphere to produce more physiologically normal brain activity. Future stratified analyses are required to clarify how lesion severity shapes rehabilitation-related brain plasticity following BCI-based interventions.

Limitations

This study has several limitations. First, the sample size was relatively small, and incomplete paired EEG recordings further reduced the effective sample for neurophysiological analyses, potentially limiting statistical power and generalizability. Second, the intervention period was short with only a 4-week follow-up. The long-term therapeutic durability of closed-loop BCI–iTBS remains uncharacterized. Third, subgroup analyses based on stroke subtype, anatomical lesion location, time since stroke onset, and baseline severity of motor impairment were not performed. Therefore, it remains unclear whether patients with different clinical phenotypes exhibit interindividual differences in response to closed-loop BCI-triggered iTBS. Fourth, unbalanced lesion severity between the BCI–sham and BCI–iTBS groups may confound inter-group neurophysiological comparisons. This potential confounder warrants further verification. Finally, the P300 analysis revealed no significant between-group changes, possibly owing to limitations of the cognitive task paradigm or insufficient sample size. Consequently, the neural mechanisms underlying cognitive improvement require further investigation using more

sensitive task paradigms.

Conclusions

This double-blind randomized controlled trial demonstrated that closed-loop BCI-triggered iTBS targeting the ipsilesional DLPFC produced clinically meaningful benefits in patients with stroke. These functional gains were accompanied by modulated sensorimotor cortical activation and enhanced brain-network efficiency. Collectively, closed-loop BCI-triggered iTBS represents a promising therapeutic strategy for post-stroke upper-limb neurorehabilitation. Larger studies with long-term follow-up and multimodal neural monitoring are warranted to refine stimulation targets, individualize intervention parameters, and further validate its clinical translational value.

Abbreviations

ADL	Activities of Daily Living
ARAT	Action Research Arm Test
BCI	Brain–computer interface
CT	Computed tomography
DLPFC	Dorsolateral prefrontal cortex
EEG	Electroencephalography
ERS	Event–related synchronization
ERD	Event–related desynchronization
ERSP	Event–related spectral perturbation
FMA–UE	Fugl–Meyer Assessment–Upper Extremity
FTHUE–HK	Functional Test for the Hemiplegic Upper Extremity in Hong Kong
ICA	Independent component analysis
iTBS	Intermittent theta–burst stimulation
LI	Laterality index
MA	Motor attempt
MBI	Modified Barthel Index
MI	Motor imagery
MMSE	Mini–Mental State Examination
MoCA	Montreal Cognitive Assessment
MRI	Magnetic resonance imaging
NIHSS	National Institutes of Health Stroke Scale

NIBS	Non–invasive brain stimulation
PSD	Power spectral density
rMT	Resting motor threshold
SAFE	Shoulder Abduction and Finger Extension Score
SMA	Supplementary motor area
TMS	Transcranial magnetic stimulation
wPLI	Weighted phase–lag index

Acknowledgments

The authors gratefully acknowledge the participants and clinical staff for their invaluable contributions to this study. We also thank Shanghai Idea Interaction Technology Co., Ltd. for providing technical support for the closed-loop BCI-triggered iTBS technology.

Author contributions

Conception and design: G.Y., L.M.L., and Q.S.R.. Collection of data: L.M.L., L.J., Z.R.T., L.Y.J., and Q.S.R.. Data analysis: Y.G., M.L., L.C.Y., Manuscript writing: Y.G., M.L., L.C.Y.. Critical and intellectual revision of manuscript: all authors. Final approval of manuscript: all authors. All authors read and approved the final manuscript.

Sources of Funding

This study was supported by the National Natural Science Foundation of China (82102664), Nanjing Medical University Gusu College Natural Science Foundation Project (GSKY202610510), and the Suzhou Basic Applied Research Fund of Healthcare Innovation key project (SYW2026012).

Data availability

The data analyzed during the current study are available from the corresponding author on reasonable request.

Declarations

Ethics approval and consent to participate

This study was conducted in accordance with the Declaration of Helsinki and approved by the Ethics Committee of Suzhou Municipal Hospital (Approval No. J-2025-020-K01) . Written informed consent was obtained from all participants or their immediate legal guardians before enrollment.

Competing Interests

The authors declare that they have no competing financial interests or personal relationships that could be perceived to have influenced the work reported in this paper.

Consent for publication

Not applicable.

References

1. Yang S, Deng M, Ren X, Wang F, Kong Z, Luo J, et al. Global burden of disease study highlights the global, regional and national trends of stroke. J Neurol Neurosurg Psychiatry. 2025;97:13–24. https://doi.org/10.1136/jnnp-2025-335954.

2. GBD 2021 Global Sepsis Collaborators. Global, regional, and national sepsis incidence and mortality, 1990-2021: a systematic analysis. Lancet Glob Health. 2025;13:e2013–e2026. https://doi.org/10.1016/S2214-109X(25)00356-0.

3. Lai S-M, Studenski S, Duncan PW, Perera S. Persisting consequences of stroke measured by the stroke impact scale. Stroke. 2002;33:1840–4. https://doi.org/10.1161/01.STR.0000019289.15440.F2.

4. Kimberley TJ, Cramer SC, Wolf SL, Liu C, Gochyyev P, Dawson J, et al. Long-term outcomes of vagus nerve stimulation paired with upper extremity rehabilitation after stroke. Stroke. 2025;56:2255–65. https://doi.org/10.1161/STROKEAHA.124.050479.

5. Saadon-Grosman N, Loewenstein Y, Arzy S. The ‘creatures’ of the human cortical

somatosensory system. Brain Commun. 2020;2:fcaa003. https://doi.org/10.1093/braincomms/fcaa003.

6. Abdullahi A, Wong TWL, Ng SSM. Variation in the rate of recovery in motor function between the upper and lower limbs in patients with stroke: some proposed hypotheses and their implications for research and practice. Front Neurol. 2023;14:1225924. https://doi.org/10.3389/fneur.2023.1225924.

7. Cramer SC, Riley JD. Neuroplasticity and brain repair after stroke. Curr Opin Neurol. 2008;21:76–82. https://doi.org/10.1097/WCO.0b013e3282f36cb6.

8. Yan W, Lin Y, Chen Y, Wang Y, Wang J, Zhang M. Enhancing neuroplasticity for post-stroke motor recovery: mechanisms, models, and neurotechnology. IEEE Trans Neural Syst Rehabil Eng. 2025;33:1156–68. https://doi.org/10.1109/TNSRE.2025.3551753.

9. Lefaucheur JP, Aleman A, Baeken C, Benninger DH, Brunelin J, Di Lazzaro V, et al. Evidence-based guidelines on the therapeutic use of repetitive transcranial magnetic stimulation (rTMS): an update (2014-2018). Clin Neurophysiol: Off J Int Fed Clin Neurophysiol. 2020;131:474–528. https://doi.org/10.1016/j.clinph.2019.11.002.

10. Attal N, Poindessous-Jazat F, De Chauvigny E, Quesada C, Mhalla A, Ayache SS, et al. Repetitive transcranial magnetic stimulation for neuropathic pain: a randomized multicentre sham-controlled trial. Brain. 2021;144:3328–39. https://doi.org/10.1093/brain/awab208.

11. Kubis N. Non-invasive brain stimulation to enhance post-stroke recovery. Frontiers in Neural Circuits. 2016;10. https://doi.org/10.3389/fncir.2016.00056.

12. Xia X, Kang X, Jia L, Wang Q, Zhang L, Zhang R, et al. Intermittent theta burst stimulation enhances the efficacy of brain–computer interface in upper limb rehabilitation post-stroke. Front Neurol. 2026;17:1839697. https://doi.org/10.3389/fneur.2026.1839697.

13. Chung SW, Hill AT, Rogasch NC, Hoy KE, Fitzgerald PB. Use of theta-burst stimulation in changing excitability of motor cortex: a systematic review and meta-analysis. Neurosci Biobehav Rev. 2016;63:43–64. https://doi.org/10.1016/j.neubiorev.2016.01.008.

14. Bütefisch CM, Weβling M, Netz J, Seitz RJ, Hömberg V. Relationship between interhemispheric inhibition and motor cortex excitability in subacute stroke patients. Neurorehabil Neural Repair. 2008;22:4–21. https://doi.org/10.1177/1545968307301769.

15. McDonnell MN, Stinear CM. TMS measures of motor cortex function after stroke: a meta-analysis. Brain Stimul. 2017;10:721–34. https://doi.org/10.1016/j.brs.2017.03.008.

16. Alawieh A, Zhao J, Feng W. Factors affecting post-stroke motor recovery: implications on neurotherapy after brain injury. Behav Brain Res. 2018;340:94–101. https://doi.org/10.1016/j.bbr.2016.08.029.

17. Fisicaro F, Lanza G, Grasso AA, Pennisi G, Bella R, Paulus W, et al. Repetitive transcranial magnetic stimulation in stroke rehabilitation: review of the current evidence and pitfalls. Ther Adv Neurol Disord. 2019;12:1756286419878317. https://doi.org/10.1177/1756286419878317.

18. Hordacre B, Goldsworthy MR, Vallence A-M, Darvishi S, Moezzi B, Hamada M, et al. Variability in neural excitability and plasticity induction in the human cortex: a brain stimulation study. Brain Stimul. 2017;10:588–95. https://doi.org/10.1016/j.brs.2016.12.001.

19. Baniqued PDE, Stanyer EC, Awais M, Alazmani A, Jackson AE, Mon-Williams MA, et al. Brain-computer interface robotics for hand rehabilitation after stroke: a systematic review. J Neuroeng Rehabil. 2021;18:15. https://doi.org/10.1186/s12984-021-00820-8.

20. Chen S, Cao L, Shu X, Wang H, Ding L, Wang S-H, et al. Longitudinal Electroencephalography Analysis in Subacute Stroke Patients During Intervention of Brain–Computer Interface With Exoskeleton Feedback. Front Neurosci. 2020;14:809. https://doi.org/10.3389/fnins.2020.00809.

21. Ding Q, Lin T, Wu M, Yang W, Li W, Jing Y, et al. Influence of iTBS on the Acute Neuroplastic Change After BCI Training. Front Cell Neurosci. 2021;15:653487. https://doi.org/10.3389/fncel.2021.653487.

22. Yasen A, Sun W, Gong Y, Xu G. Progress in the combined application of Brain-Computer Interface and non-invasive brain stimulation for post-stroke motor recovery. Clinical Neurophysiology. 2025;180:2111383. https://doi.org/10.1016/j.clinph.2025.2111383.

23. Pichiorri F, Mattia D. Brain-computer interfaces in neurologic rehabilitation practice. Handb Clin Neurol. 2020;168:101–16. https://doi.org/10.1016/B978-0-444-63934-9.00009-3.

24. Brunner I, Lundquist CB, Pedersen AR, Spaich EG, Dosen S, Savic A. Brain computer interface training with motor imagery and functional electrical stimulation for patients with severe upper limb paresis after stroke: a randomized controlled pilot trial. J NeuroEngineering Rehabil. 2024;21:10. https://doi.org/10.1186/s12984-024-01304-1.

25. Biasiucci A, Leeb R, Iturrate I, Perdikis S, Al-Khodairy A, Corbet T, et al. Brain-actuated functional electrical stimulation elicits lasting arm motor recovery after stroke. Nat Commun. 2018;9:2421. https://doi.org/10.1038/s41467-018-04673-z.

26. Johnson NN, Carey J, Edelman BJ, Doud A, Grande A, Lakshminarayan K, et al. Combined rTMS and virtual reality brain–computer interface training for motor recovery after stroke. J Neural Eng. 2018;15:016009. https://doi.org/10.1088/1741-2552/aa8ce3.

27. Buch E, Weber C, Cohen LG, Braun C, Dimyan MA, Ard T, et al. Think to move: a neuromagnetic brain-computer interface (BCI) system for chronic stroke. Stroke. 2008;39:910–7. https://doi.org/10.1161/STROKEAHA.107.505313.

28. Zhan G, Chen S, Ji Y, Xu Y, Song Z, Wang J, et al. EEG-Based Brain Network Analysis of Chronic Stroke Patients After BCI Rehabilitation Training. Front Hum Neurosci. 2022;16:909610. https://doi.org/10.3389/fnhum.2022.909610.

29. Blankertz B, Sannelli C, Halder S, Hammer EM, Kubler A, Muller KR, Curio G, Dickhaus T: Neurophysiological predictor of SMR-based BCI performance. Neuroimage 2010, 51(4):1303-9. https://doi.org/10.1016/j.neuroimage.2010.03.02.

30. Chen J, Li Y, Yao S, Huang Y, Ma W, Li Z, et al. The Influence of M1 and DLPFC iTBS on BCI Performance: A TMS and fNIRS Study. Transl Stroke Res. 2026;17:29. https://doi.org/10.1007/s12975-026-01424-x.

30. Ding Q, Lin T, Wu M, Yang W, Li W, Jing Y, et al. Influence of iTBS on the Acute Neuroplastic Change After BCI Training. Front Cell Neurosci. 2021;15:653487. https://doi.org/10.3389/fncel.2021.653487.

31. Chen J, Liu Q, Chen G, Cai G, Jiang J, Yang X, et al. iTBS on RDLPFC improves performance of motor imagery: a brain-computer interface study combining EEG and fNIRS. J NeuroEngineering Rehabil. 2025;22:172. https://doi.org/10.1186/s12984-025-01688-8.

32. Wu Y, Dong Q, Chen J, Huang C, Zhang M. Temporal synchrony promotes motor recovery and ipsilesional cortical reorganization in BCI-based stroke rehabilitation: a randomized controlled trial. J NeuroEng Rehabil. 2026. https://doi.org/10.1186/s12984-026-02100-9.

33. Pernet C, Garrido MI, Gramfort A, Maurits N, Michel CM, Pang E, et al. Issues and recommendations from the OHBM COBIDAS MEEG committee for reproducible EEG and MEG research. Nat Neurosci. 2020;23:1473–83. https://doi.org/10.1038/s41593-020-00709-0.

34. Delorme A, Makeig S. EEGLAB: an open source toolbox for analysis of single-trial EEG dynamics including independent component analysis. J Neurosci Methods. 2004;134:9–21. https://doi.org/10.1016/j.jneumeth.2003.10.009.

35. Anthony J B, Terrence J S. An information-maximization approach to blind separation and blind deconvolution. Neural Comput. 1995 Nov;7(6):1129-59. https://doi.org /10.1162/ neco. 1995.7.6.1129.

36. Pion Tonachini L, Kreutz Delgado K, Makeig S. ICLabel: an automated electroencephalographic independent component classifier, dataset, and website. Neuroimage. 2019;198:181–97. https://doi.org/10.1016/j.neuroimage.2019.05.026.

37. Welch P. The use of fast fourier transform for the estimation of power spectra: a method based on time averaging over short, modified periodograms. IEEE Trans Audio Electroacoust. 1967;15:70–3. https://doi.org/10.1109/TAU.1967.1161901.

38. Vinck M, Oostenveld R, van Wingerden M, Battaglia F, Pennartz CMA. An improved index of phase-synchronization for electrophysiological data in the presence of volume-conduction, noise and sample-size bias. Neuroimage. 2011;55:1548–65. https://doi.org/10.1016/j.neuroimage.2011.01.055.

39. Grandchamp R, Delorme A. Single-trial normalization for event-related spectral decomposition reduces sensitivity to noisy trials. Front Psychol. 2011;2:236. https://doi.org/10.3389/fpsyg.2011.00236.

40. Pfurtscheller G, Lopes da Silva FH. Event-related EEG/MEG synchronization and desynchronization: basic principles. Clin Neurophysiol. 1999;110:1842–57. https://doi.org/10.1016/S1388-2457(99)00141-8.

41. Torrence C, Compo GP. A practical guide to wavelet analysis. Bull Am Meteorol Soc. 1998;79:61–78. https://doi.org/10.3200/JMBR.38.2.139-159.

42. Cohen MX. Analyzing neural time series data: theory and practice. The MIT Press; 2014. https://doi.org/10.7551/mitpress/9609.001.0001.

43. Kappenman ES, Farrens JL, Zhang W, Stewart AX, Luck SJ. ERP CORE: an open resource for human event-related potential research. Neuroimage. 2021;225:117465. https://doi.org/10.1016/j.neuroimage.2020.117465.

44. Polich J. Updating P300: an integrative theory of P3a and P3b. Clinical Neurophysiology. 2007;118:2128–48. https://doi.org/10.1016/j.clinph.2007.04.019.

45. Benjamini Y, Hochberg Y. Controlling the false discovery rate: a practical and powerful approach to multiple testing. J R Stat Soc B. 1995;57:289–300. https://doi.org/10.1111/j.2517-6161.1995.tb02031.x.

46. Volz LJ, Sarfeld AS, Diekhoff S, Rehme AK, Pool EM, Eickhoff SB, et al. Motor cortex excitability and connectivity in chronic stroke: a multimodal model of functional reorganization. Brain Struct Funct. 2015;220(2):1093-1107 doi:10.1007/s00429-013-0702-8

47. Tianyu J, Linhong M, Chong L, Aixian L, Zhibin L, Linhong J. 5 hz rTMS improves motor-imagery based BCI classification performance. Annu Int Conf IEEE Eng Med Biol Soc. 2021;2021. https://doi.org/10.1109/EMBC46164.2021.9630102.

48. Shu X, Chen S, Chai G, Sheng X, Jia J, Zhu X. Neural Modulation By Repetitive Transcranial Magnetic Stimulation (rTMS) for BCI Enhancement in Stroke Patients. Annu Int Conf IEEE Eng Med Biol Soc. 2018;2018:2272–5. https://doi.org/10.1109/EMBC.2018.85128

60.

49. Afonso M, Sánchez Cuesta F, González Zamorano Y, Pablo Romero J, Vourvopoulos A. Investigating the synergistic neuromodulation effect of bilateral rTMS and VR brain-computer interfaces training in chronic stroke patients. J Neural Eng. 2024;21:056037. https://doi.org/10.1088/1741-2552/ad8836.

50. Gharabaghi A, Kraus D, Leão MT, Spüler M, Walter A, Bogdan M, et al. Coupling brain-machine interfaces with cortical stimulation for brain-state dependent stimulation: enhancing motor cortex excitability for neurorehabilitation. Front Hum Neurosci. 2014;8:122. https://doi.org/10.3389/fnhum.2014.00122.

51. Daly I, Blanchard C, Holmes NP. Cortical excitability correlates with the event-related desynchronization during brain–computer interface control. J Neural Eng. 2018;15:026022. https://doi.org/10.1088/1741-2552/aa9c8c.

52. Baxter BS, Edelman BJ, Sohrabpour A, He B. Anodal transcranial direct current stimulation increases bilateral directed brain connectivity during motor-imagery based brain-computer interface control. Front Neurosci. 2017;11:691. https://doi.org/10.3389/fnins.2017.00691.

53. Hétu S, Grégoire M, Saimpont A, Coll M-P, Eugène F, Michon P-E, et al. The neural network of motor imagery: an ALE meta-analysis. Neurosci Biobehav Rev. 2013;37:930–49. https://doi.org/10.1016/j.neubiorev.2013.03.017.

54. Oostra KM, Van Bladel A, Vanhoonacker ACL, Vingerhoets G. Damage to fronto-parietal networks impairs motor imagery ability after stroke: a voxel-based lesion symptom mapping study. Front Behav Neurosci. 2016;10:5. https://doi.org/10.3389/fnbeh.2016.00005.

55. Martel M, Glover S. TMS over dorsolateral prefrontal cortex affects the timing of motor imagery but not overt action: further support for the motor-cognitive model. Behav Brain Res. 2023;437:114125. https://doi.org/10.1016/j.bbr.2022.114125.

56. Kurkin S, Gordleeva S, Savosenkov A, Grigorev N, Smirnov N, Grubov VV, et al. Transcranial magnetic stimulation of the dorsolateral prefrontal cortex increases posterior theta rhythm and reduces latency of motor imagery. Sensors. 2023;23:4661. https://doi.org/10.3390/s23104661.

855 57. Sharma N, Baron J-C, Rowe JB. Motor imagery after stroke: relating outcome to motor
856 network connectivity. Ann Neurol. 2009;66:604–16. https://doi.org/10.1002/ana.21810.

857 58. Page SJ, Fulk GD, Boyne P. Clinically important differences for the upper-extremity fugl-
858 meyer scale in people with minimal to moderate impairment due to chronic stroke. Phys Ther.
859 2012;92:791–8. https://doi.org/10.2522/ptj.20110009.

860 59. Kim MS, Park H, Kwon I, An K-O, Kim H, Park G, et al. Efficacy of brain-computer
861 interface training with motor imagery-contingent feedback in improving upper limb function
862 and neuroplasticity among persons with chronic stroke: a double-blinded, parallel-group,
863 randomized controlled trial. J Neuroeng Rehabil. 2025;22:1. https://doi.org/10.1186/s12984-
864 024-01535-2.

865 60. Li LL, Wu JJ, Li KP, Jin J, Xiang YT, Hua X-Y, et al. Comparative efficacy of different
866 noninvasive brain stimulation protocols on upper-extremity motor function and activities of
867 daily living after stroke: a systematic review and network meta-analysis. Neurol Sci.
868 2024;45:3641–81. https://doi.org/10.1007/s10072-024-07437-4.

869 61. Li D, Li R, Song Y, Qin W, Sun G, Liu Y, et al. Effects of brain-computer interface based
870 training on post-stroke upper-limb rehabilitation: a meta-analysis. J Neuroeng Rehabil.
871 2025;22:44. https://doi.org/10.1186/s12984-025-01588-x.

872 62. Fan S, Zhang J, Wu J, Zang Y, Yue J, Zhang X, et al. Individualized single-session iTBS
873 modulates functional networks and neural activation to predict cognitive gain. Neuroimage.
874 2026;334:121968. https://doi.org/10.1016/j.neuroimage.2026.121968.

875 63. Lee M, Yoon JG, Lee SW. Predicting motor imagery performance from resting-state EEG
876 using dynamic causal modeling. Front Hum Neurosci. 2020;14:321.
877 https://doi.org/10.3389/fnhum.2020.00321.

878 64. Chen S, Shu X, Jia J, Wang H, Ding L, He Z, et al. Relation between sensorimotor rhythm
879 during motor attempt/imagery and upper-limb motor impairment in stroke. Clin EEG Neurosci.
880 2022;53:238–47. https://doi.org/10.1177/15500594211019917.

881 65. Chen S, Shu X, Wang H, Ding L, Fu J, Jia J. The Differences Between Motor Attempt and
882 Motor Imagery in Brain-Computer Interface Accuracy and Event-Related Desynchronization
883 of Patients With Hemiplegia. Front Neurorobot. 2021;15:706630.
884 https://doi.org/10.3389/fnbot.2021.706630.

885 66. Kaiser V, Daly I, Pichiorri F, Mattia D, Müller Putz GR, Neuper C. Relationship Between
886 Electrical Brain Responses to Motor Imagery and Motor Impairment in Stroke. Stroke.
887 2012;43:2735–40. https://doi.org/10.1161/STROKEAHA.112.665489.

888 67. Gerloff C, Bushara K, Sailer A, Wassermann EM, Chen R, Matsuoka T, et al. Multimodal
889 imaging of brain reorganization in motor areas of the contralesional hemisphere of well
890 recovered patients after capsular stroke. Brain. 2006;129 Pt 3:791–808.
891 https://doi.org/10.1093/brain/awh713.

892 68. Sehm B, Perez MA, Xu B, Hidler J, Cohen LG. Functional neuroanatomy of mirroring
893 during a unimanual force generation task. Cereb Cortex. 2010;20:34–45.
894 https://doi.org/10.1093/cercor/bhp075.

69. Young BM, Nigogosyan Z, Walton LM, Remsik A, Song J, Nair VA, et al. Dose-response relationships using brain-computer interface technology impact stroke rehabilitation. Front Hum Neurosci. 2015;9:361. https://doi.org/10.3389/fnhum.2015.00361.

70. Young BM, Nigogosyan Z, Walton LM, Song J, Nair VA, Grogan SW, et al. Changes in functional brain organization and behavioral correlations after rehabilitative therapy using a brain-computer interface. Front Neuroeng. 2014;7:26. https://doi.org/10.3389/fneng.2014.00026.